Applied Ocean Research 144 (2024) 103903

Contents lists available at ScienceDirect

Applied Ocean Research

journal homepage: www.elsevier.com/locate/apor

Research paper

Implementation of digital twin-enabled virtually monitored data in inspection planning

Shen Li *, Feargal Brennan

Department of Naval Architecture, Ocean and Marine Engineering, University of Strathclyde, 16 Richmond St, Glasgow G1 1XQ, United Kingdom

ARTICLE INFO

Keywords:
Digital twin
Structural monitoring
Inspection planning
Structural integrity
Fatigue reliability

ABSTRACT

Marine structures are subjected to cyclic wave loads in ocean environments, leading to progressive forms of structural degradation such as fatigue cracks. To ensure fitness-for-service of these critical assets, there has been increasing interest in the application of digital twin-enabled virtual monitoring techniques. Whilst numerous studies have focused on computational algorithms dedicated to virtual monitoring, little effort has been devoted to establishing a practical digital-to-physical connection and decision-making based on virtually monitored data. This paper bridges this research gap by proposing an approach for implementing digital twin-enabled virtually monitored data in inspection planning for marine structures. The inspection of fatigue-prone structural components plays a crucial role in structural integrity management. Reliability-informed inspection, which employs a probabilistic approach that prioritises inspections based on probability of failure, offers a cost-effective approach by avoiding unnecessary inspections and reducing life-cycle costs. However, conducting a comprehensive structural reliability analysis requires thorough knowledge of the actual operational profile and current state of a structure (e.g. consumed fatigue life) in order to accurately predict its future performance (e.g. remaining fatigue life). Although design specifications and assumptions can serve as guidelines, a high degree of uncertainty may arise due to the discrepancy between the actual operational profile and the design assumptions. The approach developed in this paper consists of four main elements: virtual monitoring, data-driven forecasting, fatigue reliability, and inspection planning. This provides a practical means for establishing a connection between condition monitoring and assessment in the digital world and decision-making in the physical world. An illustrative numerical example is then presented to demonstrate the application of the proposed framework. Finally, avenues for future research and developments in this field are discussed.

1. Introduction

Structural integrity management is crucial for the safety and fitness-for-service of marine structures throughout their service life. The typical phases of structural integrity management are data, evaluation, strategy and programme (O'Connor et al., 2005). Structural monitoring has become a prevalent approach for acquiring the condition data of in-service structures, facilitating integrity analysis and supporting decision-making. Within the field of structural monitoring, digital twin is an emerging approach and has gained significant attention from both academia and industry in the recent years (Wagg et al., 2020; VanDerHorn and Mahadevan, 2021; Tuegel et al., 2011). A framework of digital twin-enabled structural integrity management was proposed by Li and Brennan (2024), an overview of which is shown in Fig. 1. In principle, digital twin serves as the counterpart of physical structures in a digital world by capturing parameters such as scantling, material properties, and degradation at both macro and micro levels, and can accurately predict structural response and damage under a given scenario. Twinning refers to the process of reducing the uncertainty between the physical structures and its digital counterpart. This is achieved by updating the digital counterpart using real-time monitored data which effectively eliminates the modelling assumptions. There are three key enabling techniques employed in digital twin: (1) digital model updating, (2) virtual monitoring, (3) data-driven forecasting. These, however, primarily focus on how real-time data and information from the physical domain are fed into the digital domain; they do not explicitly address the feedback from the digital domain to the physical domain, particularly in the context of supporting decision-making.

This paper addresses this gap by proposing an approach for the implementation of digital twin-enabled virtually monitored data in inspection planning. While digital twin-enabled monitoring provides valuable insights for structural integrity management, inspection remains an essential approach for gathering integrity-related data and

* Corresponding author.
E-mail address: shen.li@strath.ac.uk (S. Li).

https://doi.org/10.1016/j.apor.2024.103903
Received 27 July 2023; Received in revised form 24 September 2023; Accepted 22 January 2024
Available online 25 January 2024

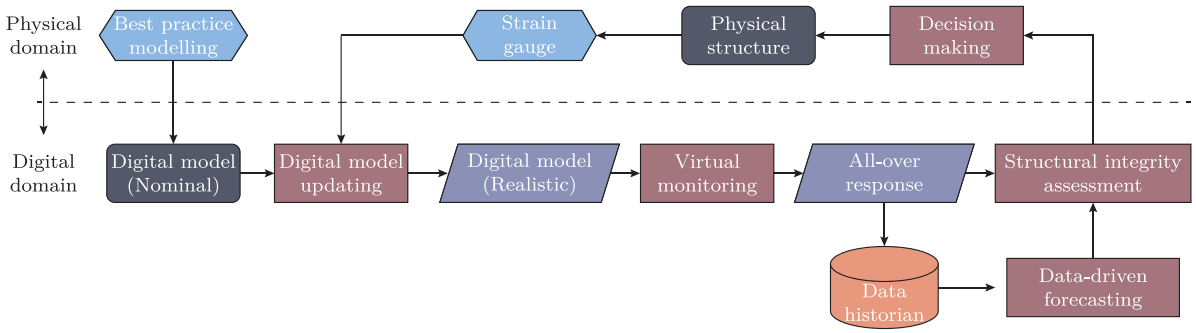

Fig. 1. Overview of digital twin-enabled structural integrity management.

complements the existing digital twin methodology. Given the high costs incurred, it is important to plan the process of inspection in a rational way. However, the stochastic nature of structural degradation (e.g., fatigue) creates significant uncertainty regarding when and where the degradation occurs. In view of this, leveraging the comprehensive information provided by the digital twin has the potential to enhance the prediction of the degradation process and subsequent decision-making (Lotsberg and Sigurdsson, 2014).

The remainder of this paper is organised as follows. A review of related works is presented in Section 2, followed by an overview of the developed approach and the fundamentals of analysis methods in Section 3. Thereafter, an illustrative example is given in Section 4 to demonstrate the capability of the developed framework. Concluding remarks are then presented in Section 5.

2. Related works

2.1. Digital twin-enabled virtual monitoring

The concept of twinning has its roots in the NASA's Apollo program where a physical twin rather than a digital twin, was built to allow mirroring the in-service space vehicle (Rosen et al., 2015). This allowed the engineers to test and assess recovery strategy on earth prior to providing instruction to the crew. It is generally recognised that the initial concept of the digital twin was introduced by Michael Grieves at the University of Michigan during executive product life-cycle management (PLM) courses (Fu, 2017). At that time, the concept was known as "mirrored spaces model" (Grieves, 2005) but was later referred as "information mirroring model" (Grieves, 2006). The concept was further expanded by Grieves (2011), introducing the term "digital twin".

In the field of marine structures, numerous studies have been reported in open literature on the development and application of digital twin to support structural integrity management for fatigue-prone components (Thompson, 2020; Hageman and Thompson, 2022; Aarsnes et al., 2019; Sireta and Storhaug, 2022; Henkel et al., 2020; Augustyn et al., 2021; Sugimura et al., 2021). The methodologies proposed in these studies principally focused on data assimilation; for instance, by combining monitored data and numerical modelling using the finite element method (FEM). Two types of approaches have been investigated, which are based on different fatigue evaluation methods, namely the spectral-based approach (Wang, 2010) and time domain approach (Li et al., 2013). In the spectral-based approach, research has mostly been dedicated to the update of operational profile (e.g., wave spectrum). For instance, Thompson (2020) and Hageman and Thompson (2022) proposed a framework for virtual monitoring enabled by FEM-based numerical twin and wave spectrum updated by hindcast wave data or wave data retrieved from motion data of a floater (i.e., floater as a buoy). A similar approach was adopted by Aarsnes et al. (2019) who combined the structural and hydrodynamic design models with the specific encountered wave information (which matched the Automatic Identification System [AIS]) and global wave hind cast data to allow real-time fatigue evaluation. In a similar vein, Sugimura et al. (2021) adopted the same analytical principle and utilised the wave data measured from a wave radar. Regarding the time domain approach within digital twin framework, the main challenge lies in translating limited measurements obtained from discrete locations to structural members with high criticality. For example, Sireta and Storhaug (2022) formulated a modal approach to reconstruct the structural response in time domain based on measurements from a smaller number of strain gauges. Henkel et al. (2020) adopted the modal decomposition and expansion method to extrapolate the measured response time history to locations of interests. Ziegler et al. (2019) explored the feasibility of applying linear regression and k-nearest neighbour approach to extrapolate strain gauge measurements. A novel methodology based on radial basis function to reconstruct strain field was proposed by Wang et al. (2023), which yielded good results for a highly non-linear response.

Reviews by Li and Brennan (2024) and Chen et al. (2021) provide a more comprehensive survey of the state-of-the-art regarding the use of digital twin for marine structures. In general, the development of digital twin for structural integrity management of marine structures has made significant progress. Various methodologies have been proposed to enable the virtual monitoring of structural members of high criticality. However, an important aspect that remains unaddressed is the practical interface between virtual monitoring and decision support. Whilst digital twin technology provides valuable insights into structural integrity, an effective mechanism for utilising this information in the decision-making process is yet to be established.

2.2. Inspection planning

Guidance note and recommended practice with respect to inspection planning are issued by various certification authorities such as DNV (Det Norske Veritas, 2021), BV (Bureau Veritas, 2017) and LR (Lloyd's Register, 2017). Qualitative and quantitative analyses are two commonly applied approach, each serving different purposes. The former is typically used to provide an efficient criticality ranking among a large number of structural systems/components (Ayyub et al., 2002; Kamsu-Foguem, 2016). For instance, a rule-based scoring approach was introduced by DeFranco et al. (1999) to assess the relative risk of offshore platforms posed to the operators, which was applied also by EI-Reedy (2006) and Potty and Akram (2011). In this approach, descriptive criteria are developed, scored and weighted by subject matter experts. The risk level is then categorised based on the total score and presented in the form of a risk matrix.

When determining the inspection interval, a quantitative assessment is normally required. This also allows an effective update of risk/reliability when new inspection information becomes available through reliability updating. Quantitative inspection planning was presented by Madsen (1985, 1987, 1997), Chen et al. (2011), Moan (2005), Kim and Frangopol (2011), Lotsberg et al. (2000) and Onoufriou

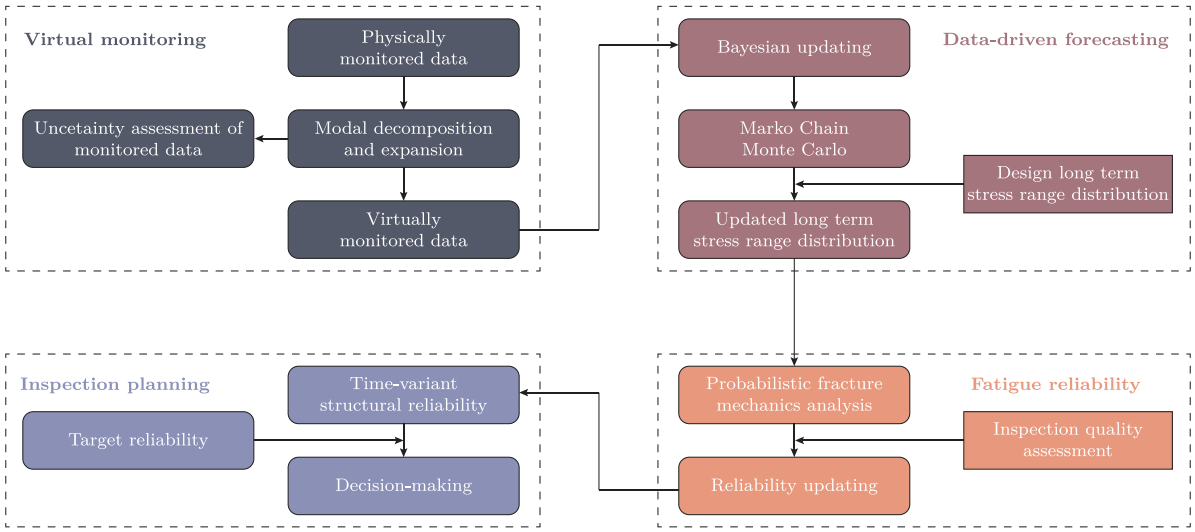

Fig. 2. Overview of implementation of digital twin-enabled virtually monitored data in inspection planning.

(1999). One of the main features of these approaches is the probabilistic fracture mechanics analysis. Using fracture mechanics rather than S-N curve to assess fatigue is preferred because the limit state function of fracture mechanics method contains the same parameter as the inspection performance model (Straub and Faber, 2006). However, the statistical information of input parameters to fracture mechanics model is not well established for marine structures, whereas the converse is the case for statistical information on the inputs for the S-N model (Lassen and Recho, 2015; Lotsberg et al., 2016). Hence, the parameters of the fracture mechanics model may require to be calibrated by S-N curves. To this end, calibrated parameters were recommended by Lotsberg and Sigurdsson (2014).

The challenge associated with quantitative risk/reliability-based assessment is that intense and specialist knowledge of probabilistic analysis is required. Driven by the need to reduce the significant computational effort which had resulted in limited application in practice, a generic approach for the risk/reliability-based inspection planning was introduced by Straub and Faber (2005, 2006). The core of this approach is to pre-establish inspection plans for generic hot spots which are deemed representative of particular hot spots in the considered structures. The inspection plan for individual hot spot is then obtained through an interpolation procedure. In addition to improving computational efficiency, the use of a generic approach enables risk/reliability-based inspection planning to be completed by non-specialist who may be unfamiliar with the probabilistic modelling of fatigue crack and reliability analysis.

3. Methodological considerations

3.1. Overview

The flow diagram in Fig. 2 presents an overview of the approach developed in this work for implementing digital twin-enabled virtually monitored data in inspection planning. It comprises four elements: virtual monitoring, data-driven forecasting, fatigue reliability and inspection planning.

Virtual monitoring is one of the core functionalities of the digital twin approach; it enables the monitoring of structural members without physical instrumentation, which distinguishes it from conventional structural monitoring. A modal decomposition and expansion method is adopted. This converts the physically monitored data into responses of any desired locations via a combination of structural mode shapes (i.e., virtual monitoring). However, there is inherent uncertainty in this process regarding measurements and selection of structural mode shape. Therefore, it is essential to perform an uncertainty assessment at this stage to avoid propagating systematic error in subsequent stages and ensuring accurate decision-making. The performance of a structural system is forecast in both the design stage (e.g total fatigue life) and in-service stage (e.g. remaining fatigue life). To facilitate this, analytical assumptions such as long-term stress range distribution need to be made. The objective of data-driven forecasting is to partially replace the adopted analytical assumption with monitored data. The Weibull distribution is a common model employed to describe the long-term stress range distribution of marine structures. For the initial design, the distribution parameters are determined empirically. In this study, Bayesian updating with Marko Chain Monte Carlo simulation is employed to update the distribution parameters using monitored data, thereby improving the prediction of fatigue loads. An assessment of fatigue reliability is then conducted to evaluate the time-variant structural reliability. The probabilistic fracture mechanics model is adopted, which can be combined with inspection quality assessment based on the probability of detection curve for specific inspection techniques. In addition, reliability updating is carried out when inspection information is available. The relation between structural reliability and in-service time provides the basis for inspection planning. Once the acceptance criteria is established (i.e., target reliability), the time interval of inspection can be determined (Lotsberg, 2016).

3.2. Digital twin enabled virtual monitoring

One of the notable advancements of digital twin-based technology is its capability to monitor the all-over response using a virtual monitoring technique (Collette et al., 2022). To achieve this, the physically monitored data are combined with the digital model using a modal decomposition and expansion theory (Henkel et al., 2020; Augustyn et al., 2021). It is assumed that the dynamics of a structure can be decomposed into an infinite number of mode shapes with different modal amplitudes:

$$\mathbf{u}(x,t) = \mathbf{\Phi}(x)\mathbf{Q}(t) \tag{1}$$

where $\mathbf{u}(x,t)$ is the dynamic structural response vector as a function of the spatial and temporal coordinates, $\mathbf{\Phi}(x) \in \mathbb{R}^{\infty}$ is the mode shape matrix and $\mathbf{Q}(t) \in \mathbb{R}^{\infty}$ is the time-varying modal amplitude vector. Let us consider the structural response of a finite number of discrete locations $(i + j)$ within the structure and partition the response into physically monitored responses, $\mathbf{u}_p(t) \in \mathbb{R}^i$ and virtually monitored responses, $\mathbf{u}_v(t) \in \mathbb{R}^j$. The aim of modal decomposition and expansion is to convert the physically monitored response into responses at unmonitored locations (which constitutes virtual monitoring).

Assuming that the structural response is governed by k structural mode shapes, a modally truncated approximation of the structural response reads:

$$\mathbf{u}(x,t)=\begin{Bmatrix}\mathbf{u}_p(t)\\ \mathbf{u}_v(t)\end{Bmatrix}=\begin{bmatrix}u_p^1(t)\\ u_p^2(t)\\ \vdots\\ u_p^i(t)\\ u_v^1(t)\\ u_v^2(t)\\ \vdots\\ u_v^j(t)\end{bmatrix}=\begin{bmatrix}\phi_p^{11} & \phi_p^{12} & \cdots & \phi_p^{1k}\\ \phi_p^{21} & \phi_p^{22} & \cdots & \phi_p^{2k}\\ \vdots & \vdots & \ddots & \vdots\\ \phi_p^{i1} & \phi_p^{i2} & \cdots & \phi_p^{ik}\\ \phi_v^{11} & \phi_v^{12} & \cdots & \phi_v^{1k}\\ \phi_v^{21} & \phi_v^{22} & \cdots & \phi_v^{2k}\\ \vdots & \vdots & \ddots & \vdots\\ \phi_v^{j1} & \phi_v^{j2} & \cdots & \phi_v^{jk}\end{bmatrix}\begin{Bmatrix}q^1(t)\\ q^2(t)\\ \vdots\\ q^k(t)\end{Bmatrix} \tag{2}$$

The modal amplitude, i.e., $\{q^1(t), q^2(t), \ldots, q^k(t)\}$, is estimated using a least-square approach as follow:

$$\tilde{\mathbf{q}}(t)=\left(\begin{bmatrix}\phi_p^{11} & \phi_p^{12} & \cdots & \phi_p^{1k}\\ \phi_p^{21} & \phi_p^{22} & \cdots & \phi_p^{2k}\\ \vdots & \vdots & \ddots & \vdots\\ \phi_p^{i1} & \phi_p^{i2} & \cdots & \phi_p^{ik}\end{bmatrix}^T\begin{bmatrix}\phi_p^{11} & \phi_p^{12} & \cdots & \phi_p^{1k}\\ \phi_p^{21} & \phi_p^{22} & \cdots & \phi_p^{2k}\\ \vdots & \vdots & \ddots & \vdots\\ \phi_p^{i1} & \phi_p^{i2} & \cdots & \phi_p^{ik}\end{bmatrix}\right)^{-1}\times\begin{bmatrix}\phi_p^{11} & \phi_p^{12} & \cdots & \phi_p^{1k}\\ \phi_p^{21} & \phi_p^{22} & \cdots & \phi_p^{2k}\\ \vdots & \vdots & \ddots & \vdots\\ \phi_p^{i1} & \phi_p^{i2} & \cdots & \phi_p^{ik}\end{bmatrix}\begin{Bmatrix}u_p^1(t)\\ u_p^2(t)\\ \vdots\\ u_p^i(t)\end{Bmatrix} \tag{3}$$

The virtually monitored response is then estimated from the following solution:

$$\begin{Bmatrix}\tilde{u}_v^1(t)\\ \tilde{u}_v^2(t)\\ \vdots\\ \tilde{u}_v^i(t)\end{Bmatrix}=\begin{bmatrix}\phi_v^{11} & \phi_v^{12} & \cdots & \phi_v^{1k}\\ \phi_v^{21} & \phi_v^{22} & \cdots & \phi_v^{2k}\\ \vdots & \vdots & \ddots & \vdots\\ \phi_v^{i1} & \phi_v^{i2} & \cdots & \phi_v^{ik}\end{bmatrix}\begin{Bmatrix}\tilde{q}^1(t)\\ \tilde{q}^2(t)\\ \vdots\\ \tilde{q}^k(t)\end{Bmatrix} \tag{4}$$

The finite element method can be employed for solving the eigenvalue problem. Nodal or elemental outputs corresponding to the desired structural location are acquired from the finite element model to formulate the mode shape matrix given in Eq. (2). This approach is an inverse problem solver, offering potential computational efficiency over direct time-domain simulations.

3.3. Uncertainty assessment of monitored data

As discussed by Hageman et al. (2022), the use of monitored data can reduce the epistemic uncertainty caused by a lack of knowledge of the actual operational and environmental conditions. However, it is equally important to recognised that uncertainty may arise from the monitoring system. There is an inevitable discrepancy between the virtually monitored response and the actual response of the physical structure. To quantify this, four uncertainty indicators may be relevant (Augustyn et al., 2021), namely the time response assurance criterion (TRAC), coefficient of determination (CoD), bias (b) and coefficient of variation (CoV). The TRAC is defined by the following expression:

$$\mathrm{TRAC}=\frac{(\mathbf{u}^T\tilde{\mathbf{u}})^2}{(\mathbf{u}^T\mathbf{u})(\tilde{\mathbf{u}}^T\tilde{\mathbf{u}})}\in[0,1] \tag{5}$$

where $\mathbf{u}$ denotes the physically monitored response and $\tilde{\mathbf{u}}$ denotes the virtually monitored response. TRAC is a measure of the temporal correlation between physically and virtually monitored data with TRAC = 1 indicating a perfect correlation and TRAC = 0 implying no correlation. Because TRAC does not account for the amplitudes of the signals, coefficient of determination (CoD) is introduced to capture the potential amplitude errors:

$$\mathrm{CoD}=1-\frac{E[(\mathbf{u}-\tilde{\mathbf{u}})^2]}{Var[\mathbf{u}]}\in[-\infty,1] \tag{6}$$

where $E[\cdot]$ denotes the expectation operator and $Var[\cdot]$ denotes the variance operator. Two further metrics, bias (b) and coefficient of variation (CoV), are introduced to evaluate the amplitude range uncertainty. Bias is defined as the expected value of the cumulative amplitude range ratios of the time series:

$$b=E\left[\frac{\Delta\mathbf{u}}{\Delta\tilde{\mathbf{u}}}\right] \tag{7}$$

where $\Delta\mathbf{u}\in\mathbb{N}^m$ is the cumulative rainflow count over physically monitored time series, $\Delta\tilde{\mathbf{u}}\in\mathbb{N}^m$ is the cumulative rainflow count over virtually monitored time series. m is the number of rainflow count bins. The coefficient of variation (CoV) is defined as the standard deviation of the cumulative amplitude range ratios for all rainflow count bins normalised to the bias:

$$\mathrm{CoV}=\frac{\sqrt{Var\left[\frac{\Delta\mathbf{u}}{\Delta\tilde{\mathbf{u}}}\right]}}{b} \tag{8}$$

3.4. Bayesian updating of stress range distribution

Forecasting the structural response (e.g., stress) and possible damage (e.g., fatigue) to support the verification of structural design adequacy and the long-term planning of inspection is an integral step in the design of engineering structures. However, forecasting at an initial design stage can only be performed by making certain assumptions such as long-term stress range distribution, denoted as $f(\Delta\sigma;\theta)$. Regarding marine structures, Weibull distribution is often adopted to model the long term stress range distribution. The derivation of parameters within these design models (i.e., θ) is usually based upon the historical data of structures with a similar configuration and operational profile. Digital twin offers an opportunity for utilising the monitored response of the structure to partly remove the analysis assumption for a specific case. Bayesian updating is arguably one of the most suitable methods for this objective (Ang and Tang, 1975).

In the Bayesian approach, the parameter to be estimated (θ) is treated as a random variable and is described by a prior distribution based on prior knowledge (Lye et al., 2021), denoted as $f'(\theta)$. New information obtained from the digital twin-based monitoring can be used to formulate the likelihood function, as given, for example, by Okasha et al. (2010):

$$L(\theta)=\prod_{i=1}^{n}f(\Delta\sigma_i|\theta) \tag{9}$$

where $f(\Delta\sigma_i|\theta)$ is the probability density function evaluated at monitored data x_i, given that the distribution parameter is θ. According to the Bayesian theorem, the posterior distribution is proportional to the product of the likelihood function and the prior distribution:

$$f''(\theta)\propto L(\theta)f'(\theta) \tag{10}$$

In the present study, a Markov Chain Monte Carlo Simulation using Metropolis-Hasting algorithm (Hastings, 1970) is employed to approximate the posterior distribution. Alternative approach such as slice sampling algorithm can also be applied, as demonstrated by Okasha and Frangopol (2012).

3.5. Probabilistic fracture mechanics model

3.5.1. Crack propagation law

The fracture mechanics approach assumes that a flaw can be idealised as a sharp tipped crack which propagates in accordance with the law relating the crack growth rate (da/dN), and the stress intensity factor range for the material containing the flaw (BS7910, 2019). The

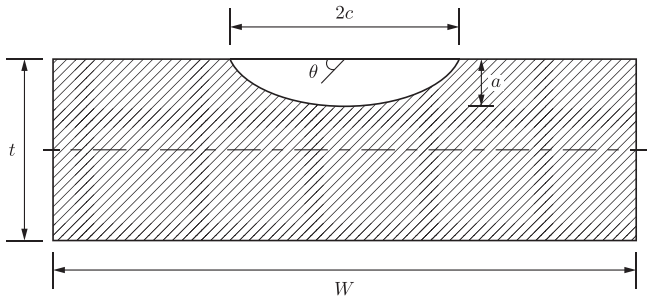

Fig. 3. Schematics of surface crack.

overall relationship between the crack growth rate and stress intensity factor range is generally a sigmoidal curve in the logarithmic scale in which the central portion may be assumed as linear such as Paris' law (Paris and Erdogan, 1963) or, for greater precision, represented by two or more straight lines. Considering a semi-elliptic surface crack with constant crack aspect ratio (Fig. 3), the following differential equation can be used to described the crack propagation:

$$\frac{da}{dN} = C(\Delta K)^m \tag{11}$$

in which a is the crack depth, ΔK is the stress intensity factor range, C and m are the crack growth parameters and da/dN is the crack growth rate with respect to number of cycle (N). $da/dN = 0$ if $\Delta K < \Delta K_{th}$ while unstable crack will develop if the maximum stress intensity factor is greater than the material fracture toughness. Integrating Eq. (11) from the initial crack size (a_0) to critical crack size (a_c) gives the total number of cycles leading to failure (total fatigue life):

$$N = \int_{a_0}^{a_c} \frac{da}{C(\Delta K)^m} \tag{12}$$

An incremental approach may also be applied when it comes to variable amplitude loading, in which the crack growth increment is estimated as follows:

$$\Delta a_i = C(\Delta K)^m \Delta N \tag{13}$$

The cumulative crack size after N cycles is then obtained as follows:

$$a_N = a_0 + \sum_{i=1}^{N} \Delta a_i \tag{14}$$

Alternatively, equivalent constant amplitude stress range can be derived from the solution of following expression (Amirafshari et al., 2021):

$$\Delta\sigma_{eq} = \left[\int_0^{\infty} \Delta\sigma^{\beta} f(\Delta\sigma) d\Delta\sigma\right]^{1/\beta} \tag{15}$$

where $f(\Delta\sigma)$ denotes the probability density function of stress range $\Delta\sigma$, β is the contribution factor and often taken as the slope of crack growth curve. Concerning a varying aspect ratio during crack growth, a two-dimensional analysis with both crack width and crack depth formulated in the fracture mechanics model should be performed. In this case, a coupled differential equation adapted from Eq. (11) is required (Straub and Faber, 2006), by which the incremental growths of crack width and depth are computed.

3.5.2. Stress intensity factor

The stress intensity factor is used to predict the stress state near the tip of a crack or notch caused by a remote load and plays a vital role in the application of linear elastic fracture mechanics (Newman and Raju, 1981). The general form of stress intensity factor solution reads as follows:

$$K = (Y\sigma)\sqrt{\pi a} \tag{16}$$

where σ is the remote stress acting on the structural member and Y is the geometry function. For fatigue analysis, the corresponding stress intensity factor range is given as:

$$\Delta K = (Y\Delta\sigma)\sqrt{\pi a} \tag{17}$$

Expression of $(Y\Delta\sigma)$ is given in BS7910 (2019) as follows:

$$(Y\Delta\sigma) = M f_w\{k_{tm} M_{km} M_m \Delta\sigma_m + k_{tb} M_{kb} M_b[\Delta\sigma_b + (k_m - 1)\Delta\sigma_m]\} \tag{18}$$

in which $\Delta\sigma_m$ is the membrane stress range, $\Delta\sigma_b$ is the bending stress range, M is the bulging correction factor, f_w is the finite width correction factor, M_{km} is the stress intensity correction factor for the membrane stress component, M_{kb} is the stress intensity correction factor for the bending stress component, k_{tm} is the membrane stress concentration factor, k_{tb} is the bending stress concentration factor, M_m is the stress intensity magnification factor, k_m is the stress concentration factor due to misalignment. For simplicity, only membrane stress is considered and a constant aspect ratio ($a/c = 0.2$) is assumed in the illustrative example given in the following section. Hence, only the formulae for M_m and M_{km} under these assumptions are provided herein while interested readers may refer to BS7910 (2019) for the complete set of expressions. The stress intensity magnification factor is given as:

$$M_m = [M_1 + M_2(a/t)^2 + M_3(a/t)^4] g_0 f_\theta / \Phi \tag{19}$$

where

$$M_1 = 1.13 - 0.09(a/c) \tag{20}$$

$$M_2 = 0.89/(0.2 + a/c) - 0.54 \tag{21}$$

$$M_3 = 0.5 - 1/(0.65 + a/c) + 14(1 - a/c)^2 4 \tag{22}$$

$$g_0 = 1 + [0.1 + 0.35(a/t)^2](1 - sin\theta)^2 \tag{23}$$

$$f_\theta = [(a/c)^2 cos^2\theta + sin^2\theta]^{0.25} \tag{24}$$

$$\Phi = \sqrt{1 + 1.464(a/c)^{1.65}} \tag{25}$$

The stress intensity correction factor is given as:

$$M_{km} = f_1 + f_2 + f_3 \tag{26}$$

where

$$f_1 = 0.43358(a/t)^{[g_1 + (g_2 a/t)^{g_3}]} + 0.93163e^{[(a/t)^{-0.050966}]} + g_4 \tag{27}$$

$$f_2 = -0.21521(1 - a/t)^{176.4199} + 2.8141(a/t)^{(-0.1074 a/t)} \tag{28}$$

$$f_3 = 0.33994(a/t)^{g_5} + 1.9493(a/t)^{0.23003} + g_6(a/t)^2 + g_7(a/t) + g_8 \tag{29}$$

The parameters $g_1, g_2, g_3, g_4, g_5, g_6, g_7$ and g_8 are estimated from the following solutions:

$$g_1 = -1.0343(a/c)^2 - 0.15657(a/c) + 1.3409 \tag{30}$$

$$g_2 = 1.3218(a/c)^{-0.61153} \tag{31}$$

$$g_3 = -0.87238(a/c) + 1.2788 \tag{32}$$

$$g_4 = -0.4619(a/c)^3 - 0.6709(a/c)^2 - 0.37571(a/c) + 4.6511 \tag{33}$$

$$g_5 = -0.015647(L/t)^3 + 0.090889(L/t)^2 - 0.1718(L/t) - 0.24587 \tag{34}$$

$$g_6 = -0.20136(L/t)^2 + 0.93311(L/t) - 0.41496 \tag{35}$$

$$g_7 = 0.20188(L/t)^2 - 0.97857(L/t) + 0.068225 \tag{36}$$

$$g_8 = -0.027338(L/t)^2 + 0.12551(L/t) - 11.218 \tag{37}$$

L in above expressions refers to the weld attachment. Also, if $M_{km} < 1$ is obtained from Eq. (26), $M_{km} = 1$ will be assumed.

3.5.3. Limit state function

In structural reliability analysis, the limit state function is defined to indicate the structural state (failure or not). In the present study, the limit state function is defined as follows:

$$G(t) = N(C, m, \Delta K, a_0) - \nu t \tag{38}$$

Table 1
Summary of parameters of probability of detection curves (NDT).

NDT technique	Description	X_0	b
UT	–	0.410	0.642
EC, MPI, ACFM	At ground welds or similar good working conditions above water	0.41	1.43
EC, MPI, ACFM	Normal working conditions above water	0.45	0.90
EC, MPI, ACFM	Underwater and less good working conditions above water	1.16	0.90

where N is the number of load cycles required for a crack to develop from initial size to critical size, ν is the mean zero up-crossing frequency and t is the time in service. $G(t) < 0$ indicates that the crack has developed to a critical size and hence failure occurs. The number of load cycles is to be determined through the approach introduced in Sections 3.5.1 and 3.5.2. To approximate the accumulated probability of failure, i.e., $P[G(t) < 0]$, a first order reliability method is adopted in this study (Melchers and Beck, 2017).

3.6. Inspection quality

There is inherent uncertainty as to whether different types of inspection will be successful (Brennan and de Leeuw, 2008). The concept of probability of detection is therefore introduced as a measure of the quality of inspection. The following sections provides more details on this concept and how it is applied in a probabilistic fracture mechanics analysis and inspection planning through reliability updating.

3.6.1. Probability of detection

Probability of detection is expressed as a function of the crack size. Trials are performed on components with known cracks for different types of Non-Destructive Testing (NDT) techniques (Dover et al., 2003). Continued efforts by ICON project towards assessing probability of detection curves for offshore structures indicate that a mean detectable depth of 1.4 to 1.8 mm if an exponential curve is assumed (Dover and Rudlin, 1996):

$$P(a) = 1 - e^{-\lambda a} \tag{39}$$

where λ is the inverse of mean detectable crack depth. Moan et al. (1997) suggested an exponential probability of detection curve with a mean detectable depth of 1.95 mm based on data from 3411 underwater NDT inspections of tubular joints in jackets. Probability of detection curves are also introduced by Det Norske Veritas (2021) for ultrasonic testing (UT), eddy current (EC), magnetic particle inspection (MPI) and alternating current field measurement (ACFM) under different working conditions. The parametric form reads as follows:

$$P(a) = 1 - \frac{1}{1 + (a/X_0)^b} \tag{40}$$

where parameters X_0 and b are curve fitted to the trail data. A summary of the two parameters for different NDT techniques are given in Table 1. Concerning visual inspection, there is little information related to probability of detection based on test data. Summarised in Table 2 are the probability of detection curves provided in Det Norske Veritas (2021) for close visual inspection. However, these are developed based on judgement rather than test data. Furthermore, while the parametric form is consistent with Eq. (40), crack width ($2c$) rather than crack depth (a) is taken as the variable. Additionally, it should be noted that the reliability of visual inspection is strongly dependent on cleaning of the inspected area. The guidance assumes that a good cleaning is performed. Thus the presented probability of detection curves for visual inspection should be used together with engineering judgement depending on actual inspection conditions such as cleaning and light conditions etc. With a good cleaning high resolution image photos are considered to qualify to the highest curve presented in Table 2.

Table 2
Summary of parameters of probability of detection curves (Visual inspection).

NDT technique	X_0	b
Easy access	15.78	1.079
Moderate access	37.15	0.954
Difficult access	83.03	1.079

3.6.2. Event margin

Event margin is defined as an indication of inspection outcome. Like the limit state event, the event of detection may be formulated as:

$$E(t) = a(t) - a_d \tag{41}$$

where a_d is the detectable size of a crack, $a(t)$ is the crack size at time t. If $E(t) < 0$, the crack size is smaller than the detectable size which means the crack will be not detected, whereas if $E(t) > 0$, the crack size is larger than the detectable size and therefore the crack will be detected. As a common approach in literature, the probability of detection curve will be treated as the probability distribution of the detectable crack size. However, Hong (1997) argued that the probability of detection is uncertain in itself and this uncertainty is not addressed by Eq. (41). To this end, the following formulation for the event of detection:

$$E(t) = \Phi^{-1}\{PoD[a(t)]\} - Z \tag{42}$$

where Z is a standard normally distributed variate and $\Phi^{-1}(\cdot)$ is the inverse of the standard normal distribution function. This formulation was extended by Straub and Faber (2006) to additionally consider the probability of false indication, that is, the probability that a defect is indicated where none is present. The concept of probability of indication was introduced:

$$PoI(a) = PoD(a) + [1 - PoD(a)]PFI \tag{43}$$

The event margin is then defined as follows:

$$E(t) = \Phi^{-1}\{PoI[a(t)]\} - Z \tag{44}$$

3.6.3. Reliability updating

With respect to damage detection, there are two possible scenarios: no detection ($E < 0$) and detection ($E > 0$). In this paper, only the first event will be considered. The probability of failure at time t following an inspection carried out at time t_1, where no crack is detected, reads as follows:

$$P(t) = P[G(t) < 0 | E(t_1) < 0] \tag{45}$$

As discussed by Jiao and Moan (1990), the probability of failure at time t conditioned on an event (e.g., inspection carried out at time t_1 where no crack is detected, $E(t_1) < 0$) can be expressed as:

$$P(t) = P[G(t) < 0 | E(t_1) < 0] = \frac{P[G(t) < 0 \cap E(t_1) < 0]}{P[E(t_1) < 0]} = \Phi(-\beta_{up}) \tag{46}$$

An approximation to the updated reliability index (β_{up}) is proposed by Terada and Takahashi (1988) as follows:

$$\beta_{up} = \frac{\beta_G - \rho A}{\sqrt{1 - \rho^2 B}} \tag{47}$$

where

$$\rho = \boldsymbol{\alpha}_G^T \boldsymbol{\alpha}_E \tag{48}$$

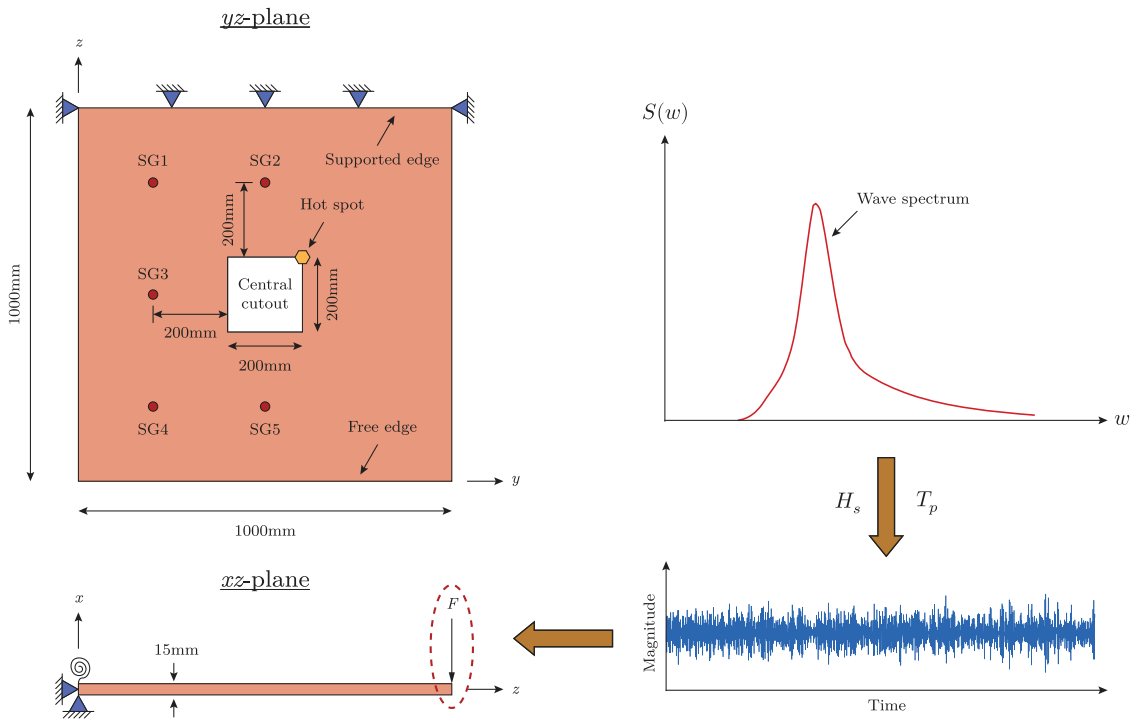

Fig. 4. Schematics of the case study model.

$$A = \phi(-\beta_E)/\Phi(-\beta_E) \tag{49}$$

$$B = A(A - \beta_E) \tag{50}$$

In above expressions, ρ is the correlation between events $G < 0$ and $E < 0$, $\phi(\cdot)$ is the standard normal density function and $\Phi(\cdot)$ is the standard normal distribution function.

For j multiple inspections without crack detection, the following formulation is derived:

$$P(t) = P[G(t) < 0 | E_1(t_1) < 0 \cap E_2(t_2) < 0 \cap \cdots \cap E_j(t_j) < 0] \tag{51}$$

The concept of equivalent event margin can be introduced which yields the same probability of failure as the original system and accounts for the correlation structure of the system (Jiao and Moan, 1990; Gollwitzer and Rackwitz, 1983).

$$P(E < 0) = P[E_1 < 0 \cap E_2 < 0 \cap \cdots \cap E_j < 0] \tag{52}$$

The equivalent reliability index is:

$$\beta_E = -\Phi^{-1}[P(E_1 < 0 \cap E_2 < 0 \cap \cdots \cap E_j < 0)] \tag{53}$$

The first order approximation of Eq. (52) is given as:

$$P(E < 0) = P[E_1 < 0 \cap E_2 < 0 \cap \cdots \cap E_j < 0] = \Phi(-\boldsymbol{\beta}; \boldsymbol{\rho}) \tag{54}$$

where $\boldsymbol{\beta} = \{\beta_1, \beta_2, \ldots, \beta_j\}^T$ is the reliability index vector and $\boldsymbol{\rho} = [\rho_{ij}]$ is the correlation matrix with $\rho_{ij} = \boldsymbol{\alpha}_i^T \boldsymbol{\alpha}_j$ for $i \neq j$ being the correlation coefficient between event margins E_i and E_j, and $\boldsymbol{\alpha}$ being the unit vector (vector of sensitivity factors) computed from first-order reliability analysis. The unit vector of the equivalent event margin ($\boldsymbol{\alpha}_E$) may be determined following the numerical procedure introduced by Gollwitzer and Rackwitz (1983):

$$\boldsymbol{\alpha}_E = \frac{\partial \beta_E / \partial \boldsymbol{U}}{\|\partial \beta_E / \partial \boldsymbol{U}\|} \tag{55}$$

where β_E is the reliability index of the equivalent event margin, $\boldsymbol{\alpha}_E$ is the unit vector of the equivalent event margin, $\boldsymbol{U}$ is the vector of standardised normal variables converted from basic variables and $\|\cdot\|$ denotes the norm of a vector. To evaluate the partial derivatives, the analytical expression based on chain rule proposed by Gong and Zhou (2017) is adopted:

$$\frac{\partial \beta_E}{\partial U_k} = e^{\frac{\beta_{ij}^2 - \beta_{E_i}^2}{2}} \Phi\left(\frac{\beta_j - \rho_{ij}\beta_i}{\sqrt{1-\rho_{ij}^2}}\right) \alpha_{k,i} + e^{\frac{\beta_{ij}^2 - \beta_{E_j}^2}{2}} \Phi\left(\frac{\beta_i - \rho_{ij}\beta_j}{\sqrt{1-\rho_{ij}^2}}\right) \alpha_{k,j} \tag{56}$$

where β_{E_i} and β_{E_j} denote the two reliability indices to be combined.

4. Illustrative example

For illustration purpose, a cantilever perforated plate under time-varying concentrated force is considered (Fig. 4). The central cutout results in stress concentration and therefore may be regarded as fatigue-prone areas with high criticality in relation to structural integrity. The objective of developing digital twin is to enable a virtual monitoring for this hot spot using the monitored data obtained from five strain gauges as indicated in Fig. 4. Although the present example is kept simple, the concepts and methodologies can be extended to the larger-scale structures instrumented with more complex monitoring system.

Data is generated through finite element numerical simulation as shown in Fig. 5. Because the data set is developed from simulation, it is effectively "simulated physically monitored data". However, for simplicity, it will be denoted as "physically monitored data" hereafter. A sequence of concentrated force is generated to represent the wave force imparted by an irregular wave train. The specific sea state under consideration is simulated through JONSWAP wave spectrum with 0.5 m significant wave height and 2.5 s peak period. For modal decomposition and expansion, four mode shapes are utilised, which a preliminary study revealed was sufficient for effective virtual monitoring.

4.1. Results

Because numerical simulation is conducted in this study for data generation, the responses of the entire plate can be obtained. A comparison of the actual response of the defined hot spot area (denoted as "physical") and the response estimated from the modal decomposition and expansion approach (denoted as "virtual") is presented in Fig. 6.

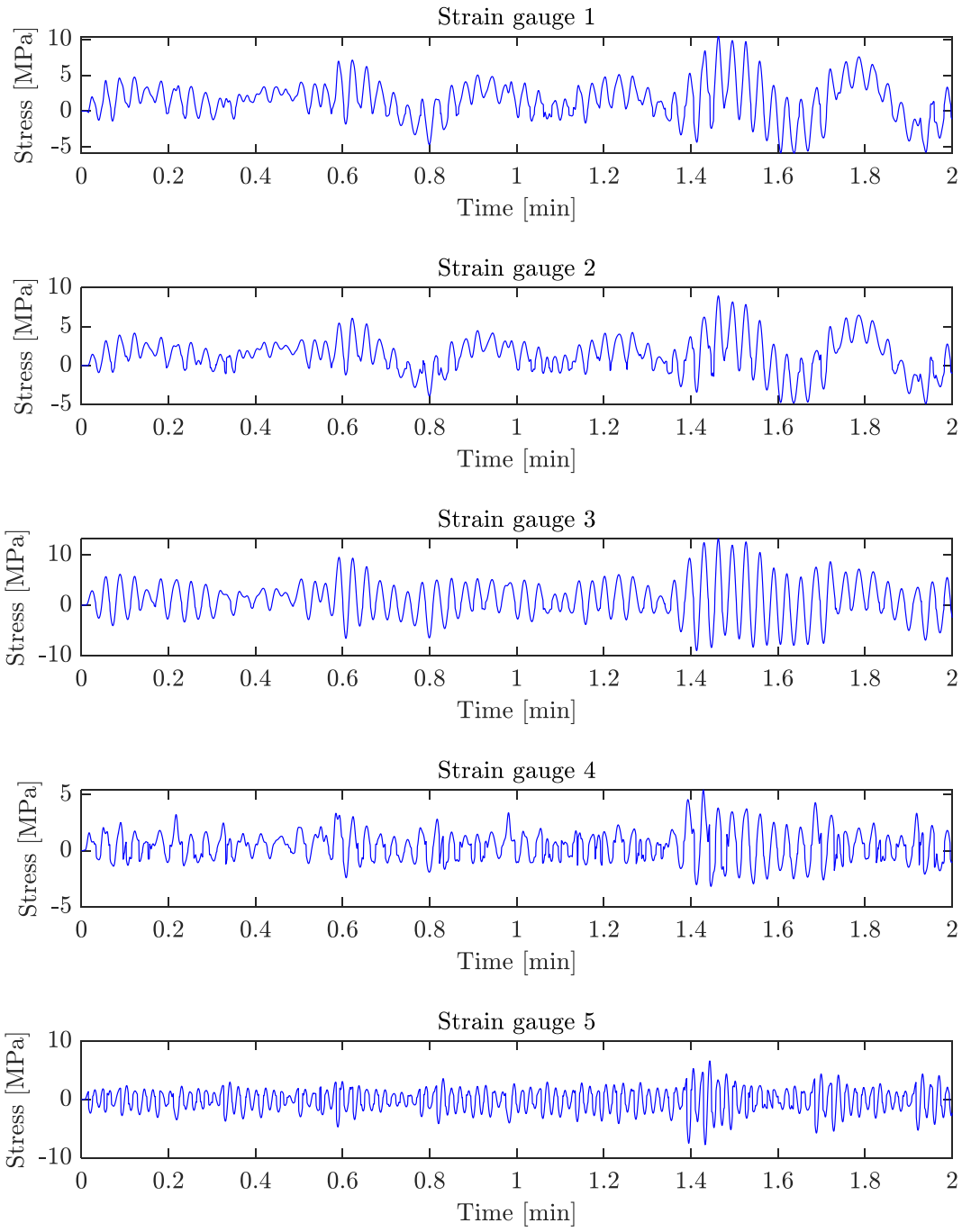

Fig. 5. "Simulated" physically monitored data.

Test case 1 refers to the use of first-order, third-order, fourth-order and sixth-order mode shapes, while test case 2 refers to the application of first-order, second-order, third-order and fourth-order mode shapes. Reasonable comparison of the time history is seen in both cases with the test case 2 experiencing greater deviation. This is further quantified through the four uncertainty indicators as illustrated in Fig. 7. Although TRAC and CoD are closed in both cases, there is appreciable difference in bias and CoV which are the uncertainty indicators related to amplitude range. In the test case 1, the virtually monitored response exhibits a higher correlation and smaller variation with the physically monitored response in terms of amplitude range than it does in test case 2. As discussed in previous section, data quality check and uncertainty assessment are essential to avoid significant errors propagating into the latter stage that will affect the decision-making (Michalak, 2023). Assuming that the uncertainty evaluation result is sufficiently representative across all the hot spots under consideration, a plausible procedure could be splitting the physically monitored dataset into a training set and a testing set, where the former is used in the modal decomposition and expansion approach and the latter is used to assess the uncertainty embedded in the virtual monitoring.

Comparisons between the prior distribution of scale parameter of Weibull distribution and its posterior estimated by MCMC are depicted in Figs. 8 and 9. Additionally, Figs. 10 and 11 compares the prior and posterior distributions of the Weibull distribution, which describes the long-term stress range distributions. Virtually monitored data of test case 1 is used in updating the scale parameter, for which normal distributions with a mean of 20 and a coefficient of variation (CoV) of 15% (Scenario 1) and normal distributions with a mean of 10 and a

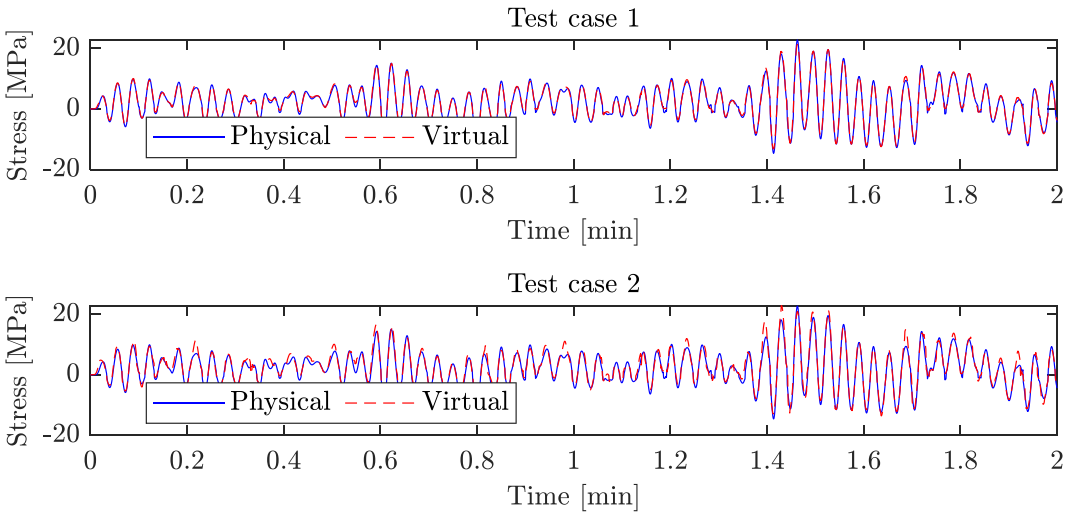

Fig. 6. A comparison of physically and virtual monitored stress series for the hot spot under consideration.

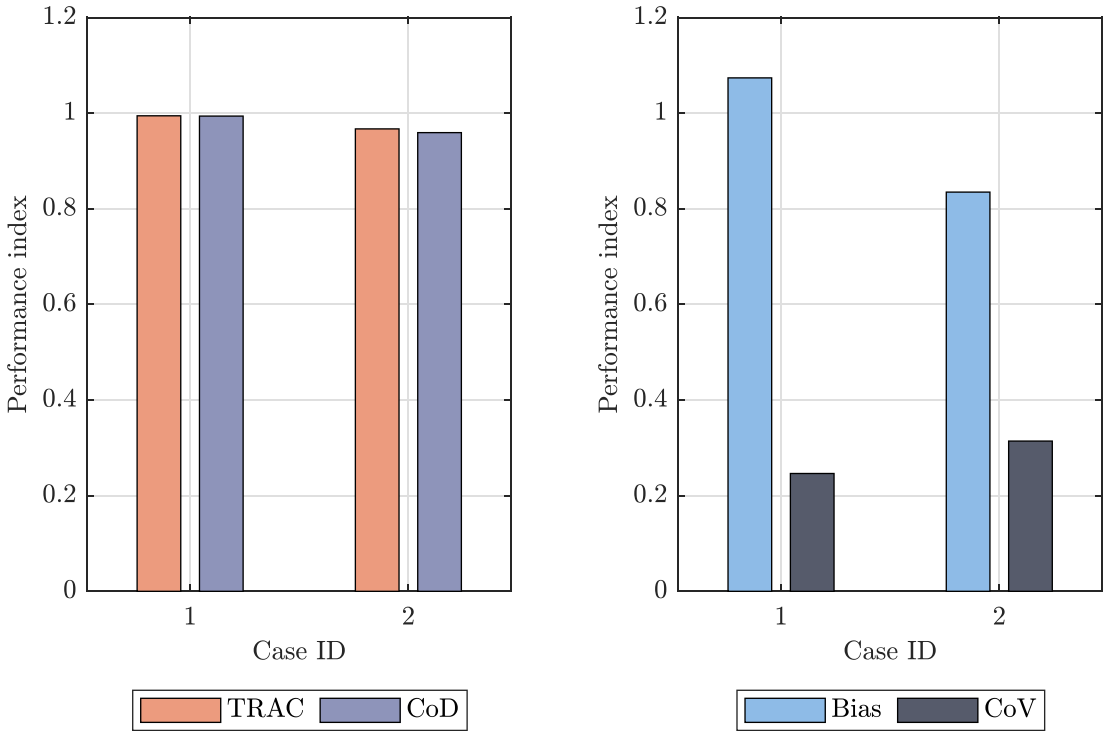

Fig. 7. Comparison of uncertainty indicators.

coefficient of variation (CoV) of 15% (Scenario 2) are assumed as the prior distribution. The two scenarios represent conservative and optimistic prior assumption, respectively. Apart from a significant change in the mean value, the uncertainty of scale parameter (characterised by CoV) is also substantially reduced.

The updated long-term stress range distribution is used in conjunction with the probabilistic fracture mechanics model. For comparison, computation is also performed using the initial design long-term stress range distribution. A summary of the input parameters is given in Table 3. The time-variant reliability indices are compared in Figs. 12 and 13 for evaluations based upon design assumption and digital twin-enabled virtually monitored data. Regarding scenario 1, it is clear that the evaluation based on design long term stress range distribution is significantly more conservative than the evaluation using digital twin-enabled virtually monitored data. For instance, to ensure reliability index is greater than the target reliability which in this example is assumed to be $\beta = 3$, four inspection are required within the entire design life time if the design assumption based evaluation is followed, namely when $t = 2.3$ year, $t = 4.2$ year, $t = 5.8$ year and $t = 14$ year. Note that the reliability index is updated in accordance with the approach introduced in previous section and because of the no detection assumption, the reliability index is increased after each inspection (Jiao and Moan, 1990). However, as shown by the digital twin-based evaluation, the reliability index still satisfies the acceptance criterion before $t = 6.4$ year, and another two inspections are required at $t = 11.7$ year and $t = 16.5$ year respectively. With regard to scenario 2, only one inspection is required when $t = 11.3$ year (according to design assumption based evaluation). Nevertheless, the evaluation based on digital twin-enabled virtually monitored data indicates the likely occurrence of fatigue failure.

Table 3
Summary of input parameters for probabilistic linear elastic fracture mechanics analysis.

Variable	Symbol	Unit	Distribution	Mean	Median	CoV
Weibull scale parameter (Design 1)	q	–	Normal	20		0.15
Weibull scale parameter (Design 2)	q	–	Normal	10		0.15
Weibull scale parameter (Updated 1)	q	–	Normal	14.1		0.037
Weibull scale parameter (Updated 2)	q	–	Normal	13.6		0.048
Weibull shape parameter (Lotsberg and Sigurdsson, 2014)	h	–	Deterministic	1.0		–
Crack growth parameter (Lotsberg and Sigurdsson, 2014)	m	–	Deterministic	3		–
Crack growth parameter (Lotsberg and Sigurdsson, 2014)	C	–	Deterministic	1.83×10^{-13}		–
Initial crack depth (Lotsberg and Sigurdsson, 2014)	a_0	mm	Exponential		0.03	1.0
Crack aspect ratio (Fajuyigbe and Brennan, 2021)	a_0/c_0	–	Deterministic		0.2	–
Zero up-crossing frequency (Lotsberg, 2016)	ν	Hz	Deterministic	0.159		–
Stress concentration factor	k_m	–	Normal	1		0.2
Detectable crack depth	a_d	mm	Exponential	0.2		1.0

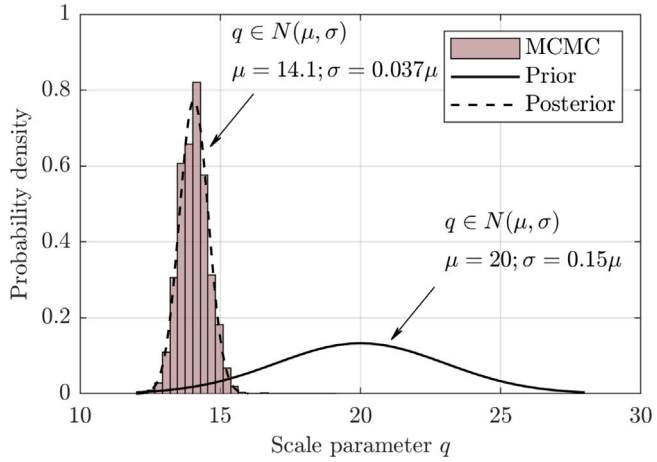

Fig. 8. Prior and posterior distribution of the scale parameter of Weibull distribution (Scenario 1).

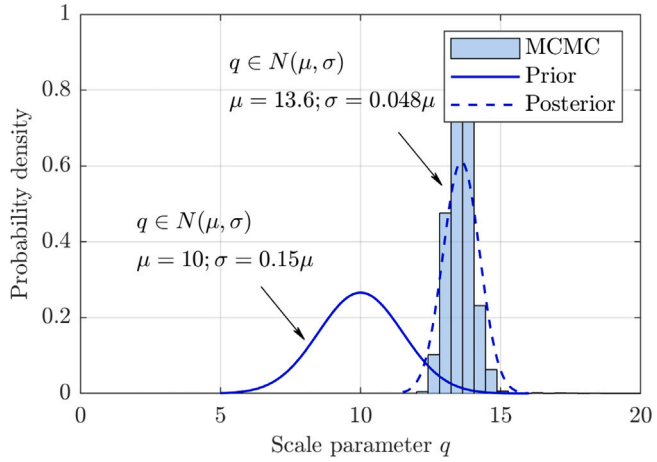

Fig. 9. Prior and posterior distribution of the scale parameter of Weibull distribution (Scenario 2).

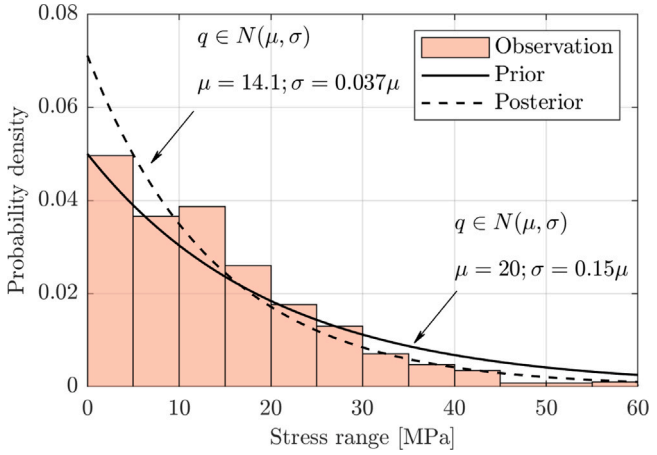

Fig. 10. Prior and posterior distribution of the Weibull stress range (Scenario 1).

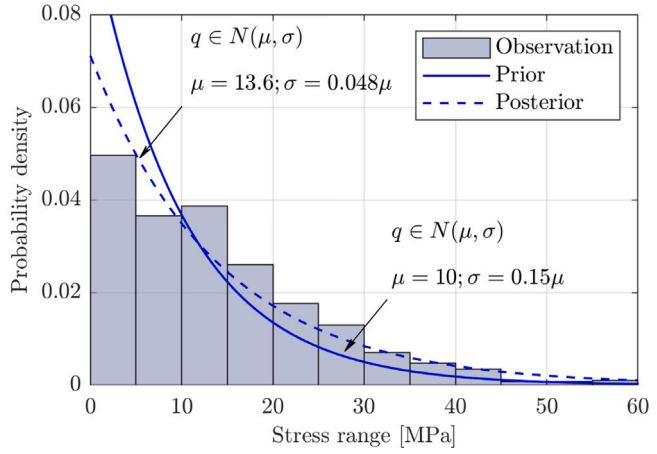

Fig. 11. Prior and posterior distribution of the Weibull stress range (Scenario 2).

A further comparison is depicted in Fig. 14 for the time-variant reliability index evaluated by virtually monitored data of test case 1 and test case 2, highlighting the influence of uncertainty in monitored data. As shown previously in Fig. 7, the virtually monitored data of test case 2 exhibits a weaker correlation with the actual response, especially in terms of amplitude range. Bayesian updating based on this series of virtually monitored data yields an updated scale parameter with mean of 11.2 and CoV of 8.19%. If this virtually monitored data is implemented in inspection planning, the first inspection is required when $t = 10.6$ year. By contrast, the use of test case 1 data, which exhibits a closer correlation with actual response, suggests that the first inspection is required at $t = 6.4$ year. Hence, significant damage or catastrophic failures may take place if the data of test case 2 were to be employed because it is likely that the structural reliability index would be substantially overestimated.

In general, the present illustrative example demonstrates the potential of digital twin-enabled virtual monitoring in optimising the inspection planning and achieving a better decision-making. When the design assumption is conservative, the use of digital twin may enable significant cost-saving associated with inspection. When the design assumption is optimistic, the use of monitoring enabled by digital twin

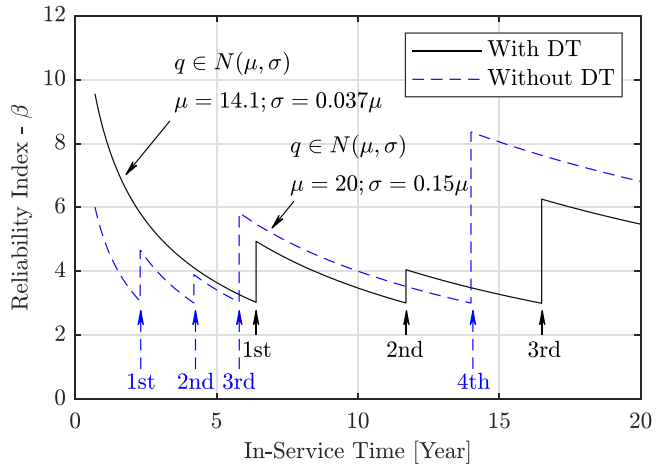

Fig. 12. Comparison of time-variant reliability index evaluated with and without digital twin enabled virtually monitored data (Scenario 1).

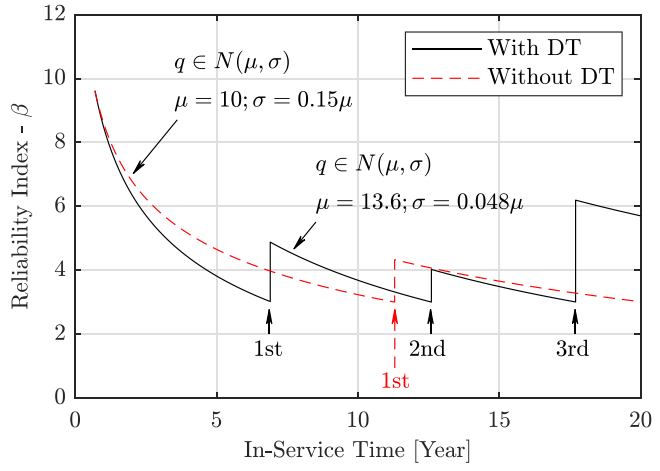

Fig. 13. Comparison of time-variant reliability index evaluated with and without digital twin enabled virtually monitored data (Scenario 2).

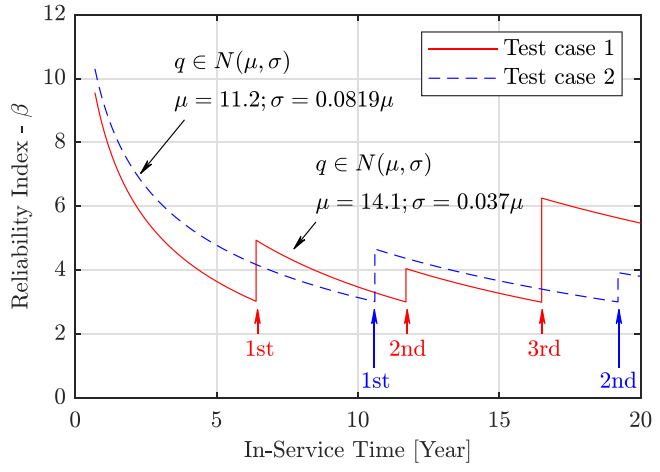

Fig. 14. Comparison of time-variant reliability index evaluated by virtually monitored data of test case 1 and 2.

represents a timely preventive intervention to avoid catastrophic failure caused by underestimation of the environmental and operational loads.

4.2. Discussions

4.2.1. Decision-making support

The present study aims to establish an approach for connecting the condition monitoring and assessment in digital domain with inspection planning in physical domain in order to leverage the capability of digital twin technology for informed decision-making. Whilst the proposed framework enhances the traditional inspection planning scheme through the implementation of digital twin-enabled virtually monitored data, a fundamental question still exists regarding the basis for decision-making support. Two scenarios are generally of relevance: application on new-built structures and application on in-service structures. The most apparent application likely pertains to structures in service, in which the monitored data can support the optimisation, re-establishment of inspection plan and demonstrate a case for life extension. The offshore wind operators are arguably the most typical examples who require life extension evaluation for the assets they manage. The recent seabed lease in Scotland for offshore wind development has a lease length of 60 years. However, offshore structures are generally designed for a much shorter service life. The introduction of monitoring system serves as a provision for the life extension of these offshore assets. Regarding new-built structures, although actual operational data is unavailable, the potential of proposed framework can be realised by using monitored data collected from prototype trials. A recent work by Branlard et al. (2023) provides a useful illustration.

4.2.2. Future works

It should be noted that the methods of analysis adopted in this study are only a subset of the various approaches available and several areas of improvements are required in future studies. Noteworthy progress has been made in data-driven forecasting (Tsai and Alipour, 2023), fatigue reliability (Wang et al., 2022; Jimenez-Martinez, 2020) and inspection planning (Yeter et al., 2020; Florian and Sørensen, 2017; Montes-Iturrizaga et al., 2008). These can positively contribute to the proposed approach.

Regarding the virtual monitoring through modal decomposition and expansion, the sensitivity of input data and structural mode shapes to the predicted responses are crucial aspects. Optimisation of sensor placement is of relevance, for which, inter alia, the studies by Yang et al. (2021), Pan et al. (2022) and Li et al. (2022) may be used as reference. Building on sensor placement optimisation, the structural mode shape may also be incorporated as a variable. Additionally, the effect of surrounding fluid on the derivation of structural mode shapes may require careful evaluation, particularly for marine structures. Another important element in the uncertainty assessment of monitored data may be the identification of erroneous physically monitored data. One viable approach is to develop a redundant setup of strain gauges that take the advantage of correlated structural response, e.g., symmetrical response (Ziegler et al., 2019). This also serves as contingency to backup the malfunctioning sensors. Additionally, correlation with other sensing units may be established; for instance SCADA data of wind turbines. Furthermore, modal decomposition and expansion can be applied within the training data set to examine their validity. With reference to the present example, the measurements of SG1, SG2, SG3 and SG4 may be utilised to predict the response at the location where SG5 is mounted. The predicted response is then compared with the physically monitored data. A significant difference may indicate a potential error in the monitoring system.

In terms of inspection planning, the illustrative example presented in this paper assumes that no crack is detected in all inspection. Nonetheless, the event of crack detection could take place in real-world inspection. To address this, a decision (event) tree approach can be adopted to combine with the present modelling. Furthermore, a set of decision rules should be specified for structural repairs when a crack is detected, such as “when structural repair should be carried out” and “how should repaired elements be treated”. With respect to the first

question, a crack depth threshold which triggers the repair should be prescribed. However, this also means that crack sizing is required in addition to detection. Alternatively, decision rule can be specified in the way that structural repair is to be carried out for all detected cracks. Concerning the latter question, a possible approach is to treat the repaired element as if no crack has been detected (Thoft-Christensen and Sørensen, 1987; Straub, 2004). This allows the development of an inspection plan for the entire or remaining lifetime of the structures, before actual inspections have been completed (i.e., pre-posterior analysis). Hence, the analysis presented in this paper can be extended to consider the events of crack detection by incorporating the desired repair strategy. After an inspection has been conducted, the inspection plan can be renewed and depending on the repair quality, a different initial crack size may be considered in the new inspection planning and pre-posterior analysis. A future study will be conducted to explore the above considerations. Another consideration that may be worthwhile to delve deeper into is the dependency between different inspections. The present work assumes statistical independency between different inspections. However, this may not hold true due to the common characteristics of environmental conditions and inspector experiences. Readers can refer to Straub and Faber (2003) for insights into the dependency effects on inspection planning.

Finally, it is important to recall that numerically generated data set is utilised in the present illustrative example. For future application in which full-scale trial data is adopted, appropriate filtering is required to reduce the impact of measurement noise. Additionally, the uncertainty checks as illustrated by Fig. 7 are highly important.

5. Concluding remarks

Digital twin concept has emerged in the recent years as a promising tool for structural integrity management. Numerous developments have been reported, accompanied by a number of algorithms focusing on data assimilation (physical-to-digital connection) However, little effort is devoted to considering the feedback from digital domain to physical domain. This paper addressed this gap by developing an approach for the implementation of digital twin-enabled virtually monitored data in inspection planning.

The developed approach incorporated four elements: virtual monitoring, data-driven forecasting, fatigue reliability and inspection planning. A modal decomposition and expansion method is adopted for virtual monitoring, through which a limited amount of monitored data taken from discrete locations can be translated to the desired structural component. With respect to data-driven forecasting, Bayesian updating based on Marko-Chain Monte Carlo is employed to facilitate the update of long-term stress range distribution specified in initial design. The fatigue reliability analysis employed a probabilistic fracture mechanics formulation and, furthermore, incorporated the inspection quality assessment through the probability of detection curve. Inspection plan was determined on the basis of the calculated time-variant reliability index and the target reliability. An illustrative example using a cantilever plate model was provided to demonstrate the fundamentals and capabilities of each element within the proposed approach. This approach thus represents a useful way to maximise the benefits of virtual monitoring enabled by digital twin and provides a technical reference for offshore asset operators with regard to the use of digital twin in structural integrity management. In addition, the example also illustrates the importance of uncertainty evaluation for the monitored data. Nevertheless, it is important to reiterate that the analytical methods adopted in this study are only a subset of the various approaches available. Further research and development will undoubtedly develop additional methodologies and advance the applications of digital twin technology in structural integrity management.

CRediT authorship contribution statement

Shen Li: Conceptualization, Methodology, Software, Validation, Formal analysis, Investigation, Data curation, Writing – original draft, Writing – review & editing, Visualization, Project administration. **Feargal Brennan:** Conceptualization, Methodology, Resources, Writing – original draft, Writing – review & editing, Supervision, Project administration, Funding acquisition.

Declaration of competing interest

No conflict of interest is declared.

Data availability

Data will be made available on request.

References

Aarsnes, L., Storhaug, G., Radon, M., 2019. Utilization of structural design models in operation to monitor fatigue strength performance. In: Practical Design of Ships and Other Floating Structures.
Amirafshari, P., Brennan, F., Kolios, A., 2021. A fracture mechanics framework for optimising design and inspection of offshore wind turbine support structures against fatigue failure. Wind Energy Sci. 6 (3), 677–699.
Ang, A.H.S., Tang, W.H., 1975. Probability Concepts in Engineering Planning and Design. John Wiley & Sons.
Augustyn, D., Pedersen, R.R., Tygesen, U.T., Ulriksen, M.D., Sørensen, J.D., 2021. Feasibility of modal expansion for virtual sensing in offshore wind jacket substructures. Mar. Struct. 79, 103019.
Ayyub, B.M., Akpan, U.O., Rushton, P.A., Koko, T.S., Ross, J., Lua, J., 2002. Risk-informed inspection for marine vessels.
Branlard, E., Jonkman, J., Brown, C., Zang, J., 2023. A digital-twin solution for floating offshore wind turbines validated using a full-scale prototype. Wind Energy Sci. 2023, 1–34.
Brennan, F., de Leeuw, B., 2008. The use of inspection and monitoring reliability information in criticality and defect assessments of ship and offshore structures. In: International Conference on Offshore Mechanics and Arctic Engineering, vol. Volume 2: Structures, Safety and Reliability, pp. 921–925.
BS7910, 2019. Guide to methods for assessing the acceptability of flaws in metallic structures.
Bureau Veritas, 2017. Risk based structural integrity management of offshore jacket structures.
Chen, B.Q., Guedes Soares, C., Videiro, P.M., 2021. Review of digital twin of ships and offshore structures. In: Maritime Technology and Engineering.
Chen, N.Z., Wang, G., Guedes Soares, C., 2011. Palmgren–Miner's rule and fracture mechanics-based inspection planning. Eng. Fract. Mech. 78 (18), 3166–3182.
Collette, M., Caridis, P., Georgiev, P., Hørte, T., Jeong, H.K., Kurt, R., Ilnytskiy, I., Okada, T., Randall, C., Sekulski, Z., Sidari, M., Zanic, V., Zhan, Z.H., Zhu, L., 2022. Committee IV.1: Design principles and criteria. In: Internatinoal Ships and Offshore Structures Congress.
DeFranco, S., O'Connor, S., Andy, T., Roy, R., Puskar, F., 1999. Development of a risk based underwater inspection process for prioritizing inspections of large numbers of platforms. In: Ocean Technology Conference.
Det Norske Veritas, 2021. Probabilistic methods for inspection planning for fatigue cracks in offshore structures DNV-RP-C210.
Dover, W.D., Brennan, F.P., Kare', R.F., Stacey, A., 2003. Inspection reliability for offshore structures. In: International Conference on Offshore Mechanics and Arctic Engineering, vol. Volume 3: Materials Technology; Ocean Engineering; Polar and Arctic Sciences and Technology; Workshops, pp. 295–299.
Dover, W., Rudlin, J., 1996. Defect characterization and classification for the ICON inspection reliability trials. In: 15th International Offshore Mechanics and Arctic Engineering.
EI-Reedy, M.A., 2006. Risk based inspection for prioritizing repair and inspections of large numbers of platforms in Gulf of Suez. In: Proceeding of 25th International Conference on Offshore Mechanics and Arctic Engineering.
Fajuyigbe, A., Brennan, F., 2021. Fitness-for-purpose assessment of cracked offshore wind turbine monopile. Mar. Struct. 77, 102965.
Florian, M., Sørensen, J.D., 2017. Risk-based planning of operation and maintenance for offshore wind farms. Energy Procedia 137, 261–272.
Fu, T.C., 2017. Navy platform digital twin.
Gollwitzer, S., Rackwitz, R., 1983. Equivalent components in first-order system reliability. Reliab. Eng. 5 (2), 99–115.
Gong, C., Zhou, W., 2017. Improvement of equivalent component approach for reliability analyses of series systems. Struct. Saf. 68, 65–72.

Grieves, M., 2005. Product lifecycle management: The new paradigm for enterprises. Int. J. Prod. Dev. 2, 71–84.
Grieves, M., 2006. Product Lifecycle Management: Driving the Next Generation of Lean Thinking. McGraw-Hill, New York.
Grieves, M., 2011. Virtually Perfect: Driving Innovative and Lean Products Through Product Lifecycle Management. Space Coast Press, Cocoa Beach, FL.
Hageman, R.B., Thompson, I., 2022. Virtual hull monitoring using hindcast and motion data to assess frigate-size vessel stress response. Ocean Eng. 245, 110338.
Hageman, R.B., van der Meulen, F.H., Rouhan, A., Kaminski, M.L., 2022. Quantifying uncertainties for Risk-Based Inspection planning using in-service Hull Structure Monitoring of FPSO hulls. Mar. Struct. 81, 103100.
Hastings, W.K., 1970. Monte Carlo sampling methods using Markov chains and their applications. Biometrika 57 (1), 97–109.
Henkel, M., Häfele, J., Weijtjens, W., Devriendt, C., Gebhardt, C., Rolfes, R., 2020. Strain estimation for offshore wind turbines with jacket substructures using dual-band modal expansion. Mar. Struct. 71, 102731.
Hong, H.P., 1997. Reliability analysis with nondestructive inspection. Struct. Saf. 19 (4), 383–395.
Jiao, G.Y., Moan, T., 1990. Methods of reliability model updating through additional events. Struct. Saf. 9 (2), 139–153.
Jimenez-Martinez, M., 2020. Fatigue of offshore structures: A review of statistical fatigue damage assessment for stochastic loadings. Int. J. Fatigue 132, 105327.
Kamsu-Foguem, B., 2016. Information structuring and risk-based inspection for the marine oil pipelines. Appl. Ocean Res. 56, 132–142.
Kim, S.Y., Frangopol, D.M., 2011. Optimum inspection planning for minimizing fatigue damage detection delay of ship hull structures. Int. J. Fatigue 33 (3), 448–459.
Lassen, T., Recho, N., 2015. Risk based inspection planning for fatigue damage in offshore steel structures. In: International Conference on Offshore Mechanics and Arctic Engineering, vol. Volume 3: Structures, Safety and Reliability.
Li, S., Brennan, F., 2024. Digital twin enabled structural integrity management: critical review and framework development. Proc. Inst. Mech. Eng. M http://dx.doi.org/10.1177/14750902241227254.
Li, S., Coraddu, A., Brennan, F., 2022. A framework for optimal sensor placement to support structural health monitoring. J. Mar. Sci. Eng. 10 (12).
Li, Z.Y., Ringsberg, J.W., Storhaug, G., 2013. Time-domain fatigue assessment of ship side-shell structures. Int. J. Fatigue 55, 276–290.
Lloyd's Register, 2017. Guidance notes for the risk based inspection of hull structures.
Lotsberg, I., 2016. Fatigue Design of Marine Structures. Cambridge University Press.
Lotsberg, I., Sigurdsson, G., 2014. A new recommended practice for inspection planning of fatigue cracks in offshore structures based on probabilistic methods. In: International Conference on Offshore Mechanics and Arctic Engineering, vol. Volume 5: Materials Technology; Petroleum Technology.
Lotsberg, I., Sigurdsson, G., Fjeldstad, A., Moan, T., 2016. Probabilistic methods for planning of inspection for fatigue cracks in offshore structures. Mar. Struct. 46, 167–192.
Lotsberg, I., Sigurdsson, G., Wold, P.T., 2000. Probabilistic inspection planning of the Åsgard a FPSO hull structure with respect to fatigue. J. Offshore Mech. Arct. Eng. 122 (2), 134–140.
Lye, A., Cicirello, A., Patelli, E., 2021. Sampling methods for solving Bayesian model updating problems: A tutorial. Mech. Syst. Signal Process. 159, 107760.
Madsen, H.O., 1985. Random fatigue crack growth and inspection. In: 7th International Conference on Structural Safety and Reliability.
Madsen, H.O., 1987. Probabilistic fatigue crack growth analysis of offshore structures with reliability updating through inspection. In: Marine Structures and Reliability Symposium.
Madsen, H.O., 1997. Stochastic modelling of fatigue crack growth and inspection. In: Probabilistic Methods for Structural Design.
Melchers, R.E., Beck, A.T., 2017. Structural Reliability Analysis and Prediction. John Wiley & Sons, Ltd.
Michalak, P., 2023. Robotics and automation are turbocharging engineering but will call for new skills. URL https://www.newcivilengineer.com/latest/robotics-and-automation-are-turbocharging-engineering-but-will-call-for-new-skills-20-06-2023/?utm_source=DSMN8&utm_medium=LinkedIn.
Moan, T., 2005. Reliability-based management of inspection, maintenance and repair of offshore structures. Struct. Infrastruct. Eng. 1 (1), 33–62.
Moan, T., Vardal, O., Hellevig, N., Skjoldli, K., 1997. In-service observations of cracks in North Sea jackets – a study on initial crack depth and POD values. In: 16th International Offshore Mechanics and Arctic Engineering.
Montes-Iturrizaga, R., Heredia-Zavoni, E., Vargas-Rodríguez, F., Faber, M.H., Straub, D., de Dios de la O, J., 2008. Risk based structural integrity management of marine platforms using Bayesian probabilistic nets. J. Offshore Mech. Arct. Eng. 131 (1).
Newman, J.C., Raju, I.S., 1981. An empirical stress-intensity factor equation for the surface crack. Eng. Fract. Mech. 15 (1), 185–192.
O'Connor, P., Bucknell, J., DeFrance, S., Westlake, H., Westlake, F., 2005. Structural integrity management (SIM) of offshore facilities. In: Offshore Technology Conference.
Okasha, N.M., Frangopol, D.M., 2012. Integration of structural health monitoring in a system performance based life-cycle bridge management framework. Struct. Infrastruct. Eng. 8 (11), 999–1016.
Okasha, N.M., Frangopol, D.M., Decò, A., 2010. Integration of structural health monitoring in life-cycle performance assessment of ship structures under uncertainty. Mar. Struct. 23 (3), 303–321.
Onoufriou, T., 1999. Reliability based inspection planning of offshore structures. Mar. Struct. 12 (7), 521–539.
Pan, Y., Ventura, C., Li, T., 2022. Sensor placement and seismic response reconstruction for structural health monitoring using a deep neural network. Bull. Earthq. Eng. 20, 4513–4532.
Paris, P., Erdogan, F., 1963. A critical analysis of crack propagation laws. J. Basic Eng. 85 (4), 528–533.
Potty, N., Akram, M., 2011. Development of a risk based underwater inspection (RBUI) methodology for Malaysia fixed offshore structure. In: Proceeding of National Postgraduate Conference.
Rosen, R., von Wichert, G., Lo, G., Bettenhausen, K., 2015. About the importance of autonomy and digital twins for the future of manufacturing. IFAC-PapersOnLine 48, 567–572.
Sireta, F., Storhaug, G., 2022. A modal approach for holistic hull structure monitoring from strain gauges measurements and structural analysis. In: Offshore Technology Conference.
Straub, D., 2004. Generic Approaches to Risk Based Inspection Planning for Steel Structures (Ph.D. thesis). ETH Zürich.
Straub, D., Faber, M.H., 2003. Modelling dependency in inspection performance. In: 9th International Conference on Applications of Statistics and Probability in Civil Engineering.
Straub, D., Faber, M.H., 2005. Risk based inspection planning for structural systems. Struct. Saf. 27 (4), 335–355.
Straub, D., Faber, M.H., 2006. Computational aspects of risk-based inspection planning. Comput.-Aided Civ. Infrastruct. Eng. 21 (3), 179–192.
Sugimura, T., Matsumoto, S., Inoue, S., Terada, S., Miyazaki, S., 2021. Hull condition monitoring and lifetime estimation by the combination of on-board sensing and digital twin technology. In: Offshore Technology Conference.
Terada, S., Takahashi, T., 1988. Failure-conditioned reliability index. J. Struct. Eng. 114 (4), 942–952.
Thoft-Christensen, P., Sørensen, J.D., 1987. Optimal strategy for inspection and repair of structural systems. Civ. Eng. Syst. 4 (2), 94–100.
Thompson, I., 2020. Virtual hull monitoring of a naval vessel using hindcast data and reconstructed 2-D wave spectra. Mar. Struct. 71, 102730.
Tsai, L.W., Alipour, A., 2023. Physics-informed long short-term memory networks for response prediction of a wind-excited flexible structure. Eng. Struct. 275, 114968.
Tuegel, E., Ingraffea, A., Eason, T., Spottswood, S., 2011. Reengineering aircraft structural life prediction using a digital twin. Int. J. Aerosp. Eng. 2011, 154798.
VanDerHorn, E., Mahadevan, S., 2021. Digital Twin: Generalization, characterization and implementation. Decis. Support Syst. 145, 113524.
Wagg, D.J., Worden, K., Barthorpe, R.J., Gardner, P., 2020. Digital twins: State-of-the-art and future directions for modeling and simulation in engineering dynamics applications. ASCE-ASME J. Risk Uncertain. Eng. Syst. Part B: Mech. Eng. 6 (3), 030901.
Wang, Y.G., 2010. Spectral fatigue analysis of a ship structural detail – A practical case study. Int. J. Fatigue 32 (2), 310–317.
Wang, B., Ke, X.G., Du, K.F., Bi, X.J., Hao, P., Zhou, C.H., 2023. A novel strain field reconstruction method for test monitoring. Int. J. Mech. Sci. 243, 108038.
Wang, L., Kolios, A., Liu, X., Venetsanos, D., Cai, R., 2022. Reliability of offshore wind turbine support structures: A state-of-the-art review. Renew. Sustain. Energy Rev. 161, 112250.
Yang, Y.C., Chadha, M., Hu, Z., Vega, M.A., Parno, M.D., Todd, M.D., 2021. A probabilistic optimal sensor design approach for structural health monitoring using risk-weighted f-divergence. Mech. Syst. Signal Process. 161, 107920.
Yeter, B., Garbatov, Y., Guedes Soares, C., 2020. Risk-based maintenance planning of offshore wind turbine farms. Reliab. Eng. Syst. Saf. 202, 107062.
Ziegler, L., Cosack, N., Kolios, A., Muskulus, M., 2019. Structural monitoring for lifetime extension of offshore wind monopiles: Verification of strain-based load extrapolation algorithm. Mar. Struct. 66, 154–163.